Diffraction imaging using partially-coherent X-rays

Harry Quiney
ARC Centre for Coherent X-ray Science
School of Physics
The University of Melbourne

4th European XFEL Users' Meeting, DESY Hamburg, 27-28 January 2010

Overview

- Fundamental elements of optical coherence theory.

- Challenges posed by imaging using partially-coherent light.

- Formulation of diffraction imaging using modal expansions.

- 1: Modal characterization of partially-coherent X-ray fields.

- 2: Imaging using a polychromatic XUV HHG source

- 3: Imaging using partially-coherent quasi-monochromatic X-rays

- 4: Imaging using a spectrally-broad synchrotron source

- Conclusion and Outlook

Optical coherence theory

Optical wavefields characterized by time-dependent electric fields, $\mathbf{E}(\mathbf{r}, t)$.

The mutual coherence is the first-order field correlation function:

$$\Gamma(\mathbf{r}_1, \mathbf{r}_2, \tau) = \langle \mathbf{E}(\mathbf{r}_1, t) \cdot \mathbf{E}^*(\mathbf{r}_2, t + \tau) \rangle$$

The Fourier transform of mutual coherence function is the cross-spectral density:

$$W(\mathbf{r}_1, \mathbf{r}_2, \omega) = \int_{-\infty}^{\infty} \Gamma(\mathbf{r}_1, \mathbf{r}_2, \tau) e^{i\omega\tau} \, d\tau.$$

Measured intensities, $I(\mathbf{r})$, are field self-correlations: $I(\mathbf{r}) = \Gamma(\mathbf{r}, \mathbf{r}, 0)$. Quasi-monochromatic approximation defines mutual optical intensity:

$$W(\mathbf{r}_1, \mathbf{r}_2, \omega) = J(\mathbf{r}_1, \mathbf{r}_2)\delta(\omega - \omega_0).$$

Paraxial propagation of $J(\mathbf{r}_1, \mathbf{r}_2)$

In the quasi-monochromatic paraxial approximation, $J(\mathbf{r}_1, \mathbf{r}_2) \mapsto J(\boldsymbol{\varrho}_1, \boldsymbol{\varrho}_2; z)$ in a plane, z, perpendicular to the direction of propagation. Then, for transverse spatial coordinates, $\boldsymbol{\varrho}_i$ and $Z = z' - z$:

$$J(\boldsymbol{\varrho}_1', \boldsymbol{\varrho}_2'; z') = \iint J(\boldsymbol{\varrho}_1, \boldsymbol{\varrho}_2; z) D(\boldsymbol{\varrho}_1', \boldsymbol{\varrho}_1, Z) D^*(\boldsymbol{\varrho}_2', \boldsymbol{\varrho}_2, Z) \, d\boldsymbol{\varrho}_1 d\boldsymbol{\varrho}_2.$$

X-ray diffraction imaging: z is at the exit surface of the scatterer, z' is the detector plane and the Fraunhofer propagation kernel is:

$$D(\boldsymbol{\varrho}', \boldsymbol{\varrho}, Z) = -\frac{i}{\lambda Z} \exp\left(-\frac{2\pi i \boldsymbol{\varrho}' \cdot \boldsymbol{\varrho}}{\lambda Z}\right)$$

If $J(\boldsymbol{\varrho}_1, \boldsymbol{\varrho}_2; z)$ represents a partially-coherent wavefield, propagation involves a four-dimensional Fourier transform.

Paraxial propagation of $J(\mathbf{r}_1, \mathbf{r}_2)$

A representative example from X-ray diffraction imaging: assume that we have

$$J(\boldsymbol{\varrho}_1, \boldsymbol{\varrho}_2; z) = \Psi(\boldsymbol{\varrho}_1)\Psi^*(\boldsymbol{\varrho}_2) \exp\left(-\frac{(\boldsymbol{\varrho}_1 - \boldsymbol{\varrho}_2)^2}{2\sigma_\ell^2}\right)$$

at the exit surface of a scattering object, where σ_ℓ is the (isotropic) coherence length. If $\sigma_\ell \to \infty$ we recover conventional coherent diffraction imaging:

$$
\begin{aligned}
I_C(\boldsymbol{\varrho}', z') &= \lim_{\sigma_\ell \to \infty} J(\boldsymbol{\varrho}', \boldsymbol{\varrho}'; z') \\
&= \mathcal{F}[\Psi(\boldsymbol{\varrho})]\mathcal{F}^{-1}[\Psi^*(\boldsymbol{\varrho})] \\
&= |\mathcal{F}[\Psi(\boldsymbol{\varrho})]|^2
\end{aligned}
$$

where $\mathcal{F}$ denotes the two-dimensional Fourier transform, and $\mathbf{u} = \boldsymbol{\varrho}'/\lambda Z$. But for finite σ_ℓ, the measured intensity is a convolution between $I_C(\mathbf{r}')$ and the correlation function, $g(\mathbf{r}_1 - \mathbf{r}_2)$.

ARC Centre of Excellence for
COHERENT X-RAY SCIENCE

The effect of partial coherence on diffraction data
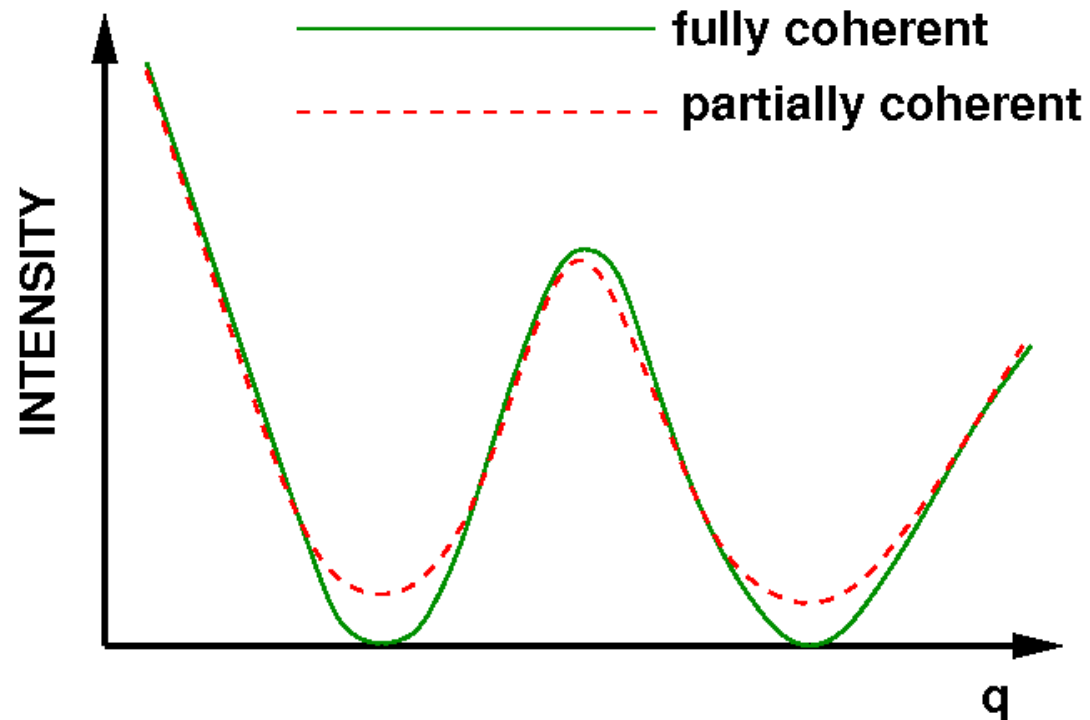
The convolution of the fully coherent intensity with $g(\mathbf{r}_1, \mathbf{r}_2)$ blurs out the intensity zeros. There exists no exit surface wave of finite spatial extent, $\Psi(\boldsymbol{\varrho})$ that satisfies $I(\boldsymbol{\varrho}') = |\mathcal{F}[\Psi(\boldsymbol{\varrho})]|^2$ and $\mathbf{u} = \boldsymbol{\varrho}'/\lambda Z$: the location of the zeros carry critical information about the support.

Fresnel imaging configuration: robustness against partial spatial coherence
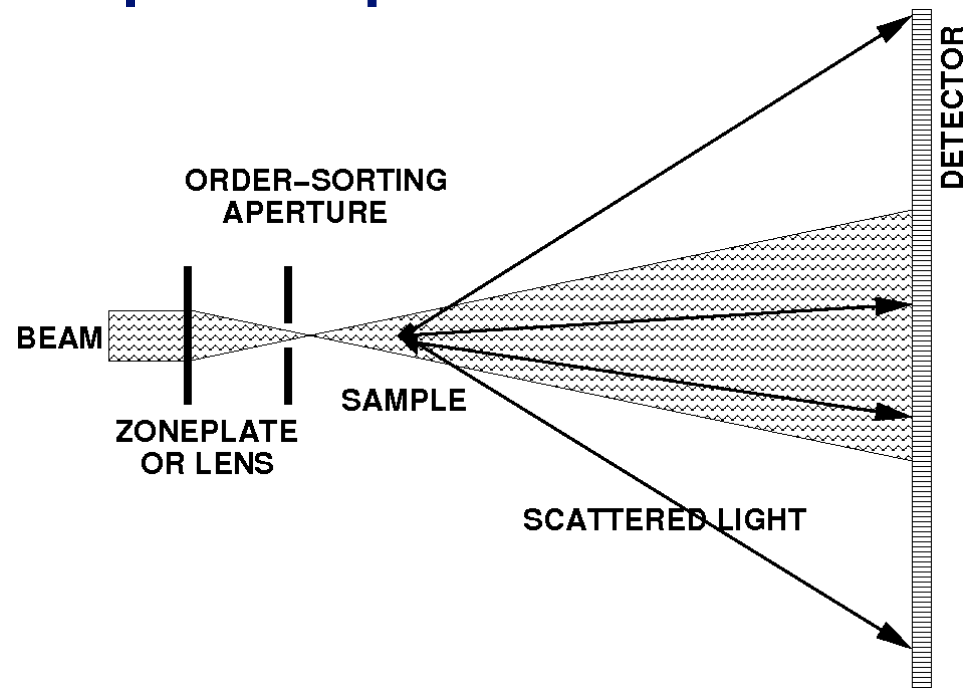
Incident phase curvature attenuates the blurring effects of a finite σ_ℓ. Fresnel coherent diffraction imaging exhibits some resistance to adverse effects of partial coherence, but is not intended as a complete remedy (Williams *et al.*, Phys. Rev. B, **75**, 104102 (2007)).

Cross-spectral density: coherent mode expansion

The Wolf coherent mode expansion represents partial spatial coherence and finite spectral width:

$$W(\mathbf{r}_1, \mathbf{r}_2, \omega) = \sum_n \alpha_n(\omega)\psi_n(\mathbf{r}_1; \omega)\psi_n^*(\mathbf{r}_2; \omega).$$

The parameters $\alpha_n(\omega)$ represent modal occupancies and are real and positive, and the orthonormal modes satisfy the Helmholtz equation

$$\left(\nabla^2 + k^2\right)\psi(\mathbf{r}; \omega) = 0$$

and the Fredholm integral equation

$$\int W(\mathbf{r}_1, \mathbf{r}_2, \omega)\psi_n(\mathbf{r}_2; \omega)d\mathbf{r}_2 = \alpha_n(\omega)\psi_n(\mathbf{r}_1; \omega)$$

Cross-spectral density: coherent mode expansion

In the quasi-monochromatic approximation, we employ the modal expansion of the mutual optical intensity:

$$I(\boldsymbol{\varrho}') = \sum_n \alpha_n \psi_n(\boldsymbol{\varrho}') \psi_n^*(\boldsymbol{\varrho}') = \sum_n \alpha_n I_n(\boldsymbol{\varrho}')$$

The incident modes and occupancies are fixed by the illumination, which we assume has been characterized by an independent measurement. The exit surface modes are $\tilde{\psi}_n(\boldsymbol{\varrho}) = T(\boldsymbol{\varrho}) \psi_n(\boldsymbol{\varrho})$ where $T(\boldsymbol{\varrho})$ is a transfer function carrying all material information about the object.

Iterative determination of $T(\boldsymbol{\varrho})$, subject to support information in the scattering plane and the measurement of $I(\boldsymbol{\varrho}')$ in the diffraction plane, $(\boldsymbol{\varrho}', z')$, preserves all useful of the information about the scattering object.

Propagation now involves a two-dimensional Fourier transform for each mode with significant occupancy.

Coherent mode expansion: imaging algorithms of partially-coherent sources

Coherent diffraction imaging algorithms iteratively determine a scalar wavefield that satisfies (a) the Helmholtz equation, (b) an amplitude constraint $I(\varrho')$ and (c) a support constraint.

For partially-coherent sources, a small number of modes are propagated between object and detector planes, subject to a knowledge of the modal occupancies (or spectral weights).

- *All* modes are scaled so that the intensity from the propagated modes matches the measured intensity

- *All* modes must satisfy the support constraint.

- Material or wavelength variation in $T(\varrho)$ must be included.

Application 1: Modal expansion of the mutual optical intensity for a synchrotron source

S. Flewett, H. M. Quiney, C. Q. Tran, K. A. Nugent, *Optics Letters*, **34**, 2198-2200 (2009).

C. Q. Tran, G. J. Williams, A. Roberts, S. Flewett, A. G. Peele, D. Paterson, M. D. de Jonge, I. McNulty, K. A. Nugent *Physical Review Letters*, **98**, 224801 (2007).

Modal expansion of the mutual optical intensity for a synchrotron source
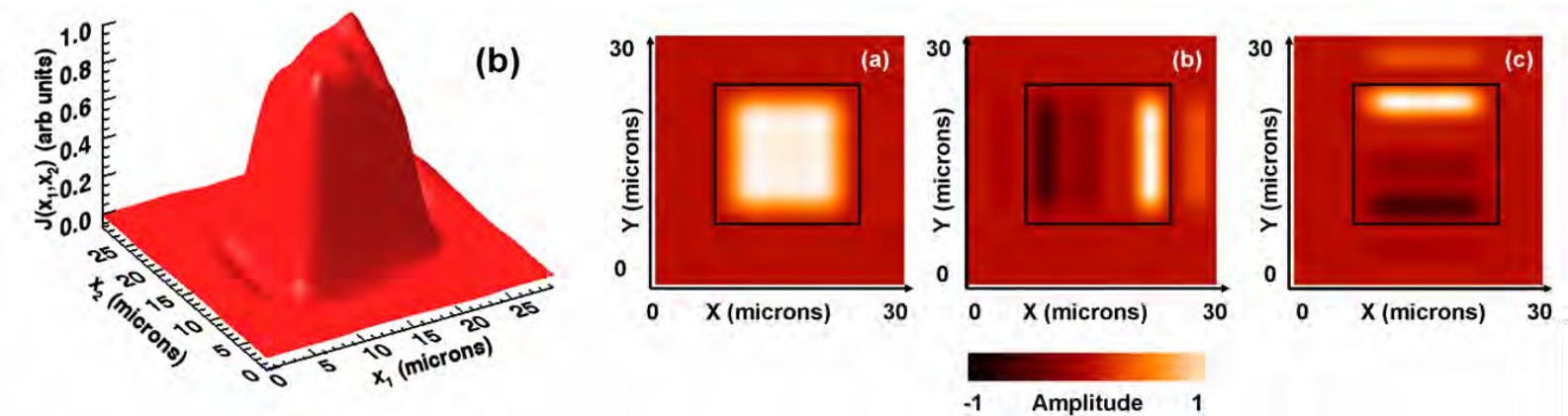
Modes fitted to a mutual optical intensity determined by phase-space tomography.

Modal occupancies: $\alpha_1 = 0.91 \pm 0.02$, $\alpha_2 = 0.04 \pm 0.02$, $\alpha_3 = 0.05 \pm 0.02$.

There is negligible contribution from higher-order modes.

Application 2: Imaging using an HHG XUV source with spectral structure

R. A. Dilanian, B. Chen, S. Teichmann, L. V. Dao, H. M. Quiney, K. A. Nugent, *Optics Letters*, **33**, 2341-2343 (2008).

B. Chen, R. A. Dilanian, S. Teichmann, B. Abbey, A. G. Peele, G. J. Williams, P. Hannaford, L. V. Dao, H. M. Quiney, K. A. Nugent, *Physical Review A*, **79**, 023809 (2009).

R. A. Dilanian, B. Chen, G. J. Williams, H. M. Quiney, K. A. Nugent, S. Teichmann, P. Hannaford, L. V. Dao, A. G. Peele, *Journal of Applied Physics*, **106**, 023110 (2009).

Imaging using an HHG XUV source with spectral structure
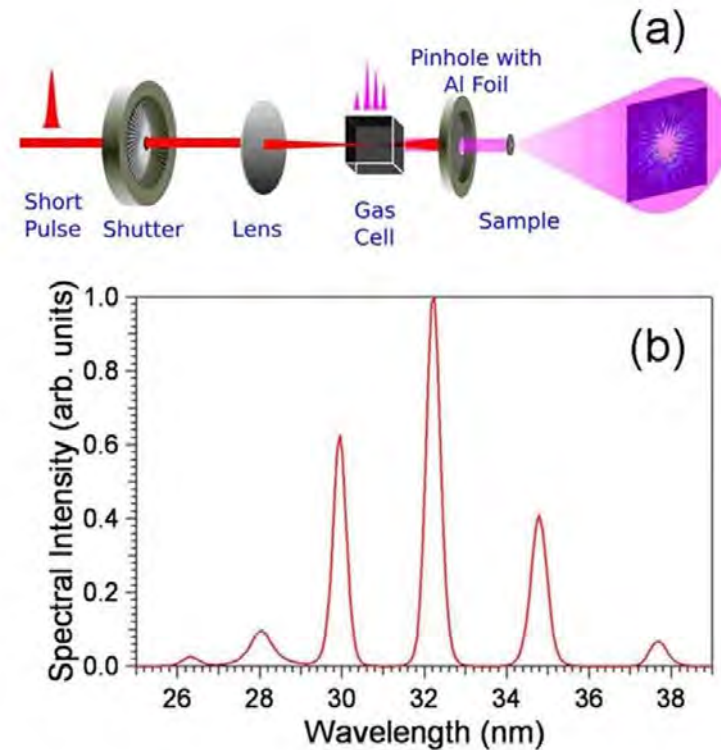
Model this HHG source by six frequency-discrete spatially-coherent modes.

Imaging using an HHG XUV source with spectral structure
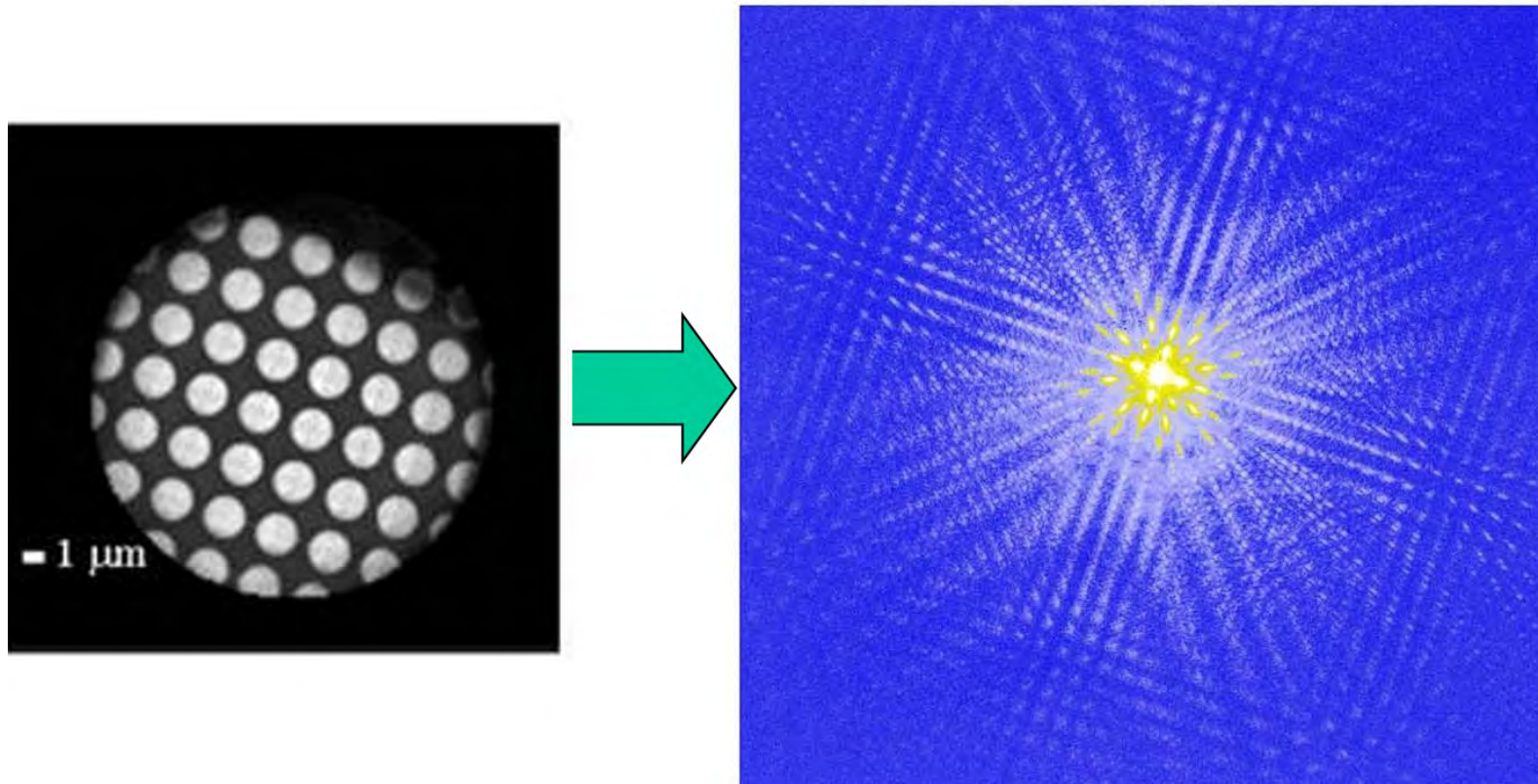
Diffraction from a carbon film target using HHG source.

Imaging using an HHG XUV source with spectral structure
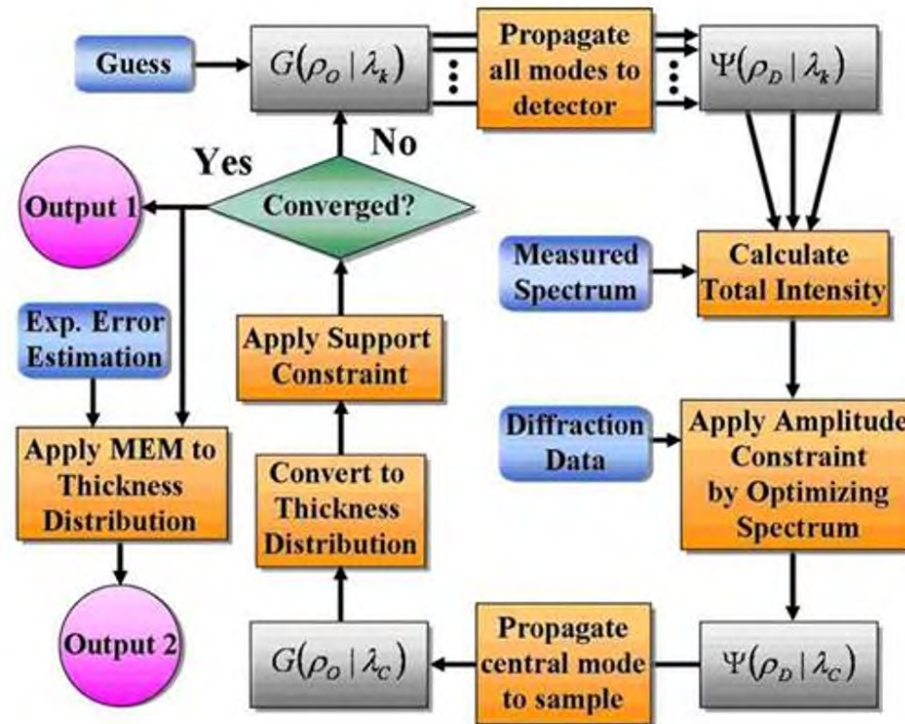
Maximum entropy refinement accommodates dependence of $T(\varrho)$ on ω.

Imaging using an HHG XUV source with spectral structure
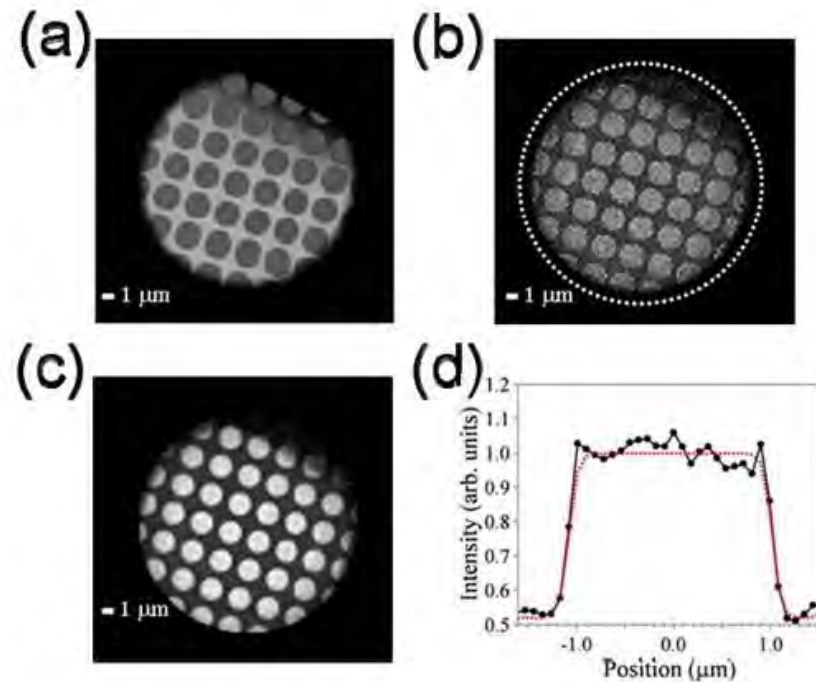
(a) microscope image of target, (b) reconstruction assuming binary $T(\varrho)$ (dotted line indicates support), (c) MaxEnt refinement including $T(\varrho, \omega)$, (d)line-out across a hole.

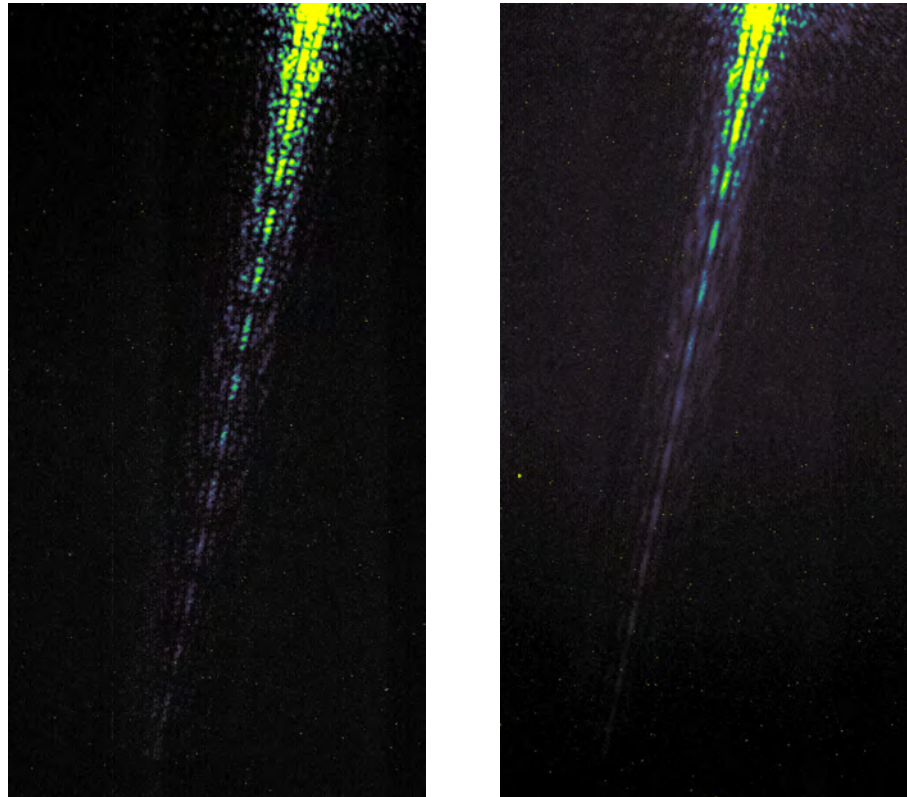# Application 3: Imaging using a partially-coherent quasi-monochromatic synchrotron source

L. W. Whitehead, G. J. Williams, H. M. Quiney, D. J. Vine, R. A. Dilanian, S. Flewett, K. A. Nugent, A. G. Peele, E. Balaur, I. McNulty, "Diffractive Imaging Using Partially Coherent X-Rays", *Physical Review Letters*, **103**, 243902, (2009).

L. W. Whitehead, G. J. Williams, H. M. Quiney, K. A. Nugent, A. G. Peele, D. Peterson, M. D. de Jong, I. McNulty, *Phys. Rev. B*, **77**, 104112 (2008).

Imaging using a partially-coherent quasi-monochromatic synchrotron source
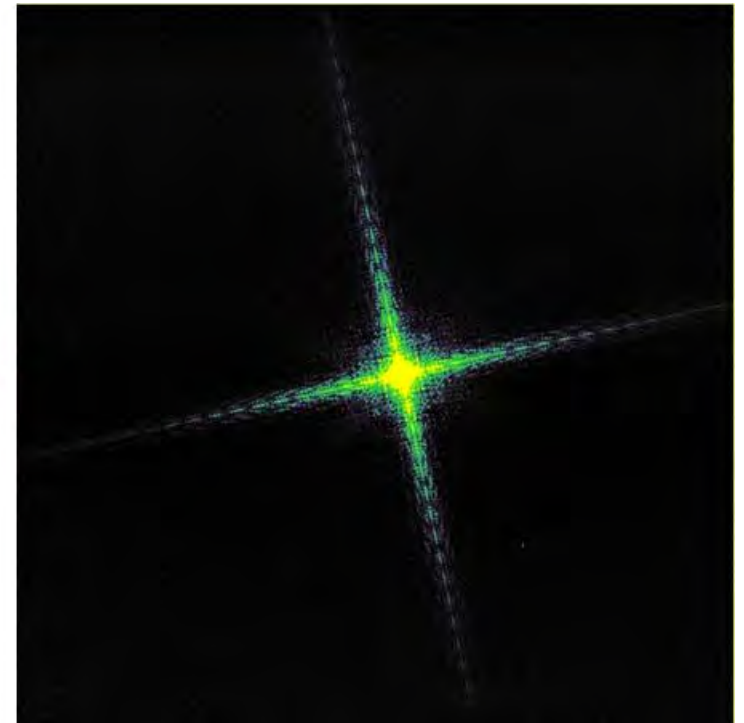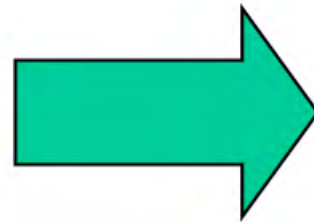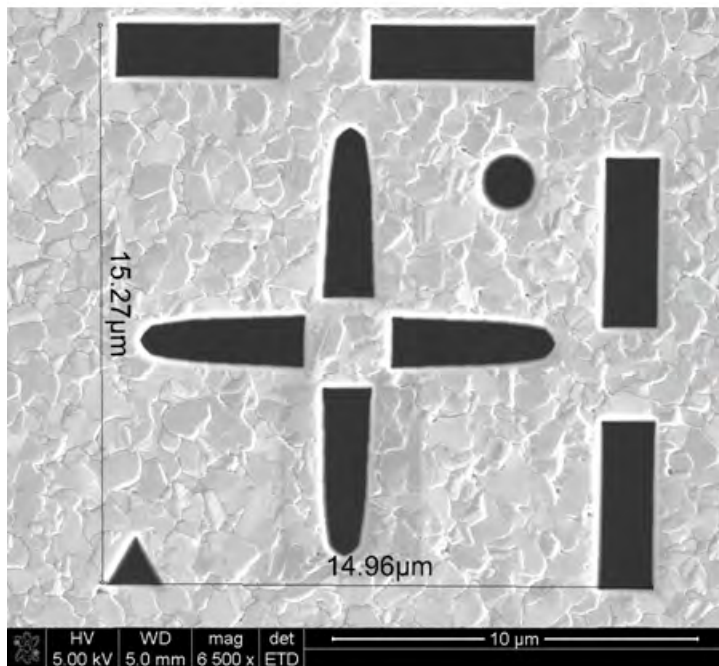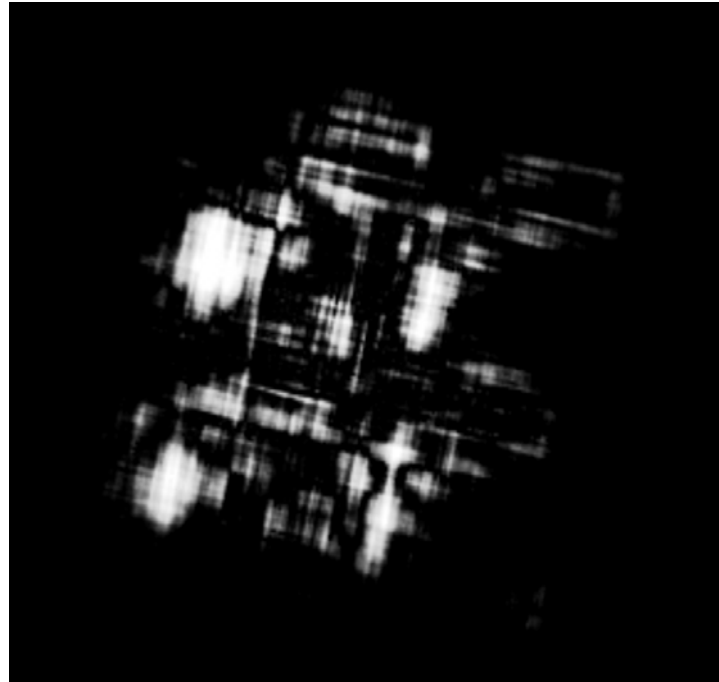
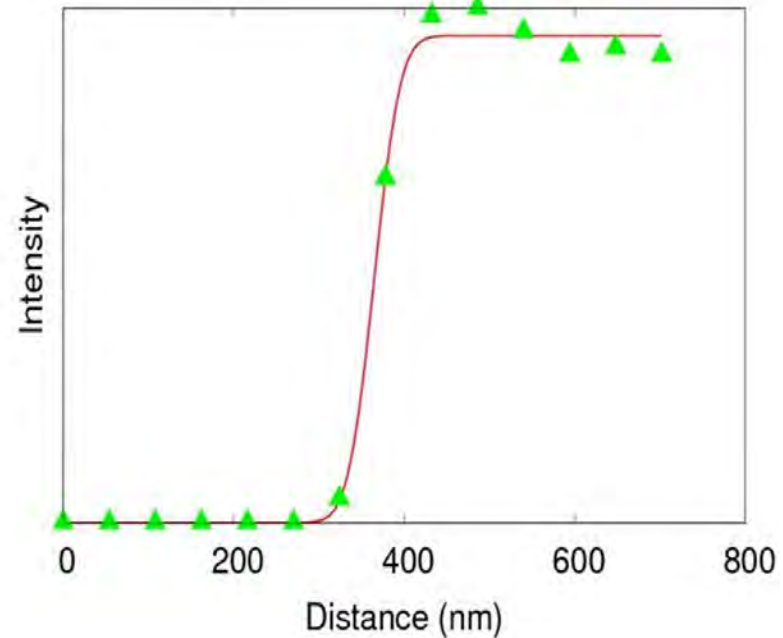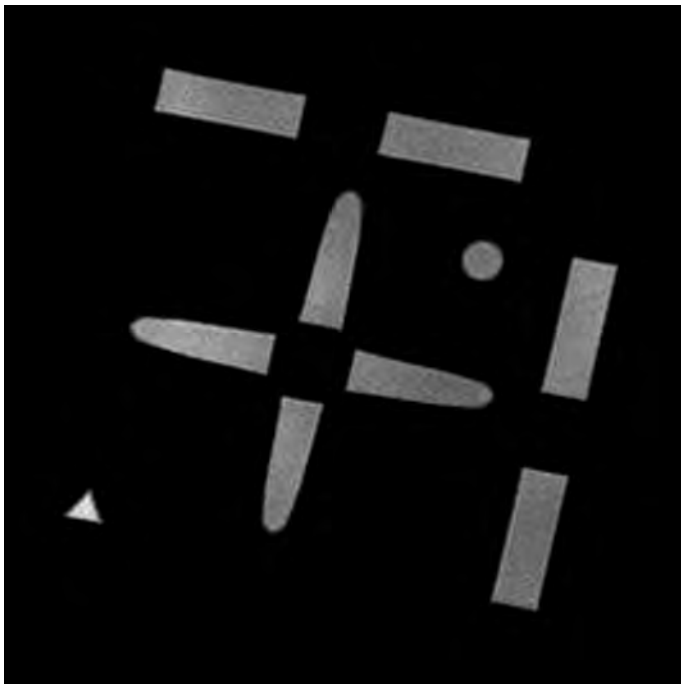# Imaging using a partially-coherent quasi-monochromatic synchrotron source

Close up of diffraction flares: high coherence (left), low coherence (right).

Imaging using a partially-coherent quasi-monochromatic synchrotron source


The straightforward application of conventional coherent diffraction imaging algorithms fail completely. The partial spatial coherence of the source has blurred the data so much that the positions of the diffraction zeros are lost.

Imaging using a partially-coherent quasi-monochromatic synchrotron source

Reconstruction from low-coherence data (left) with a line-out across the edge of a feature (right).

# Imaging using a partially-coherent quasi-monochromatic synchrotron source
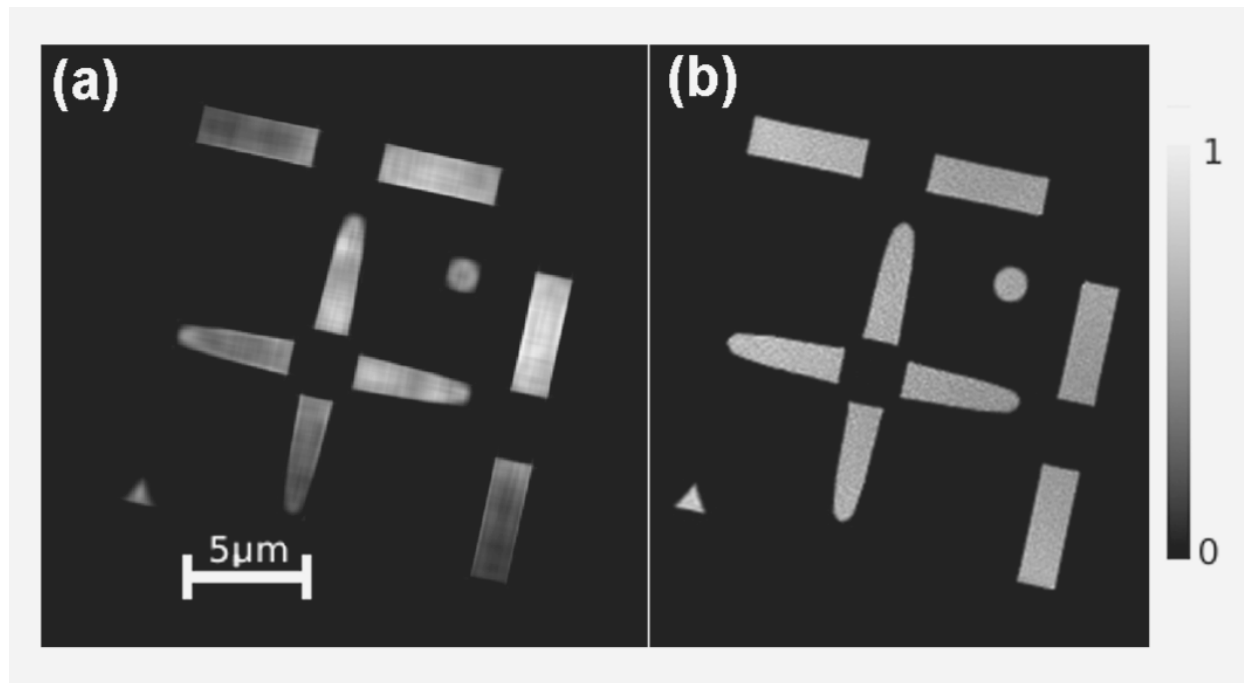
High coherence data: Conventional CDI (left) compared with three-mode expansion (right). The improvement highlights the sensitivity of CDI to even small amount of partial coherence in illumination.

Application 4: Imaging with a spectrally broad synchrotron source
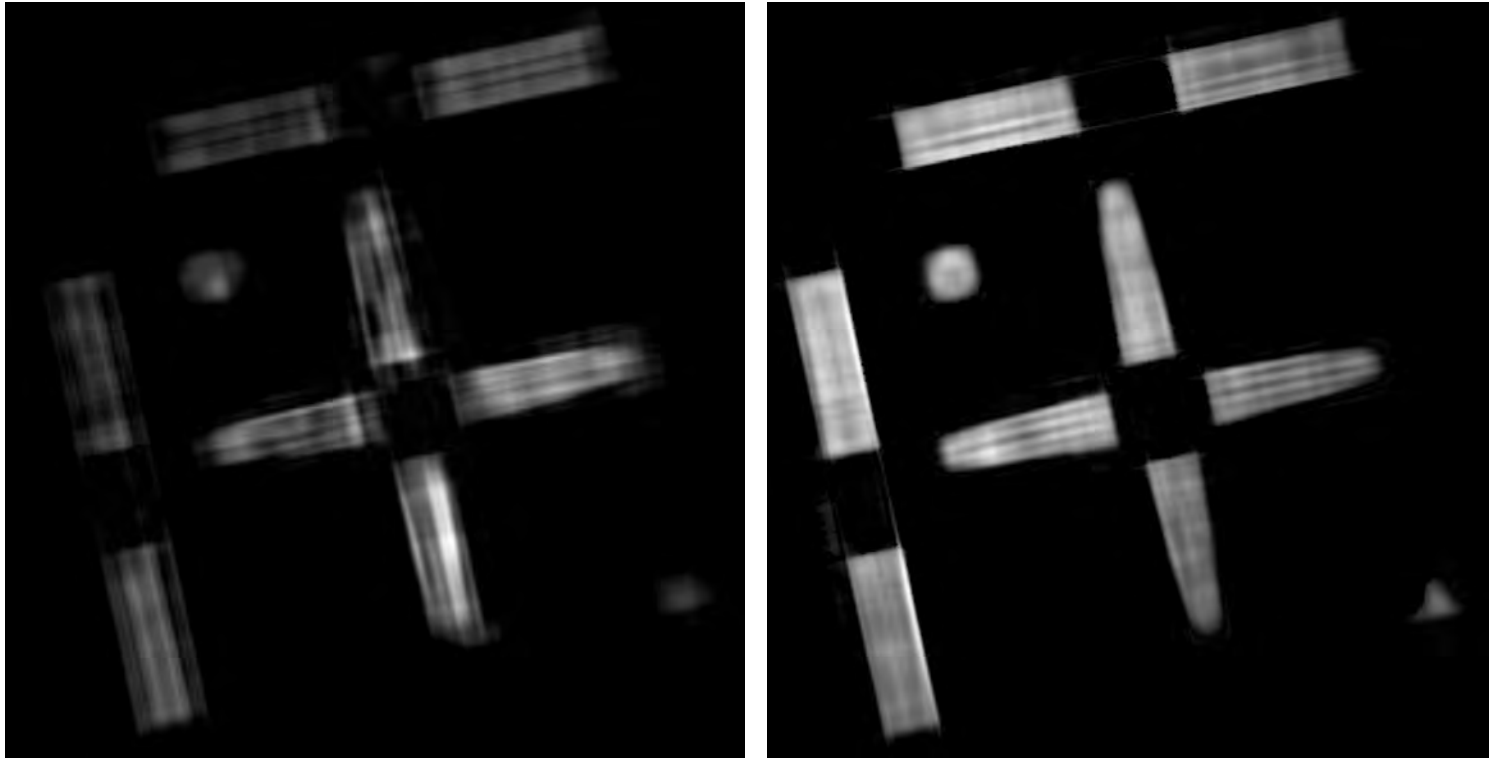
L. W. Whitehead, H. M. Quiney, K. A. Nugent (in preparation, 2010)

# Imaging with a spectrally broad synchrotron source
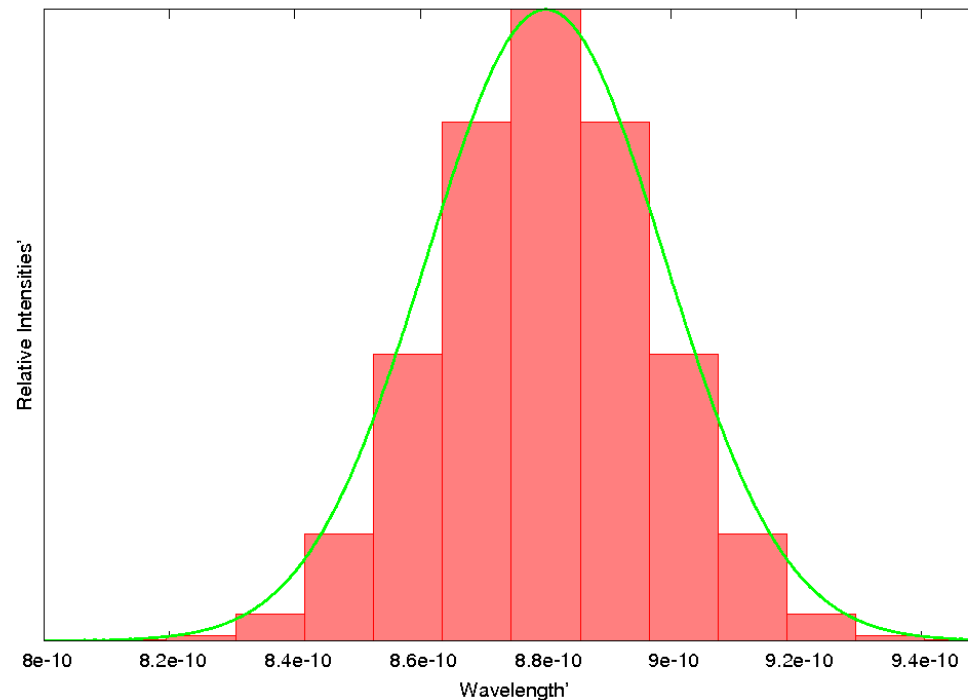
Model this third-generation synchrotron source by eleven frequency-weighted spatially-coherent modes. Finer frequency sampling cannot be resolved in the diffraction experiment.

Imaging with a spectrally broad synchrotron source

Reconstructions obtained using conventional CDI and (left) a loose support and (right) a tight support. Repeated ghosts are clearly present in the left-hand image; non-uniformities in the right-hand image.

Imaging with a spectrally broad synchrotron source
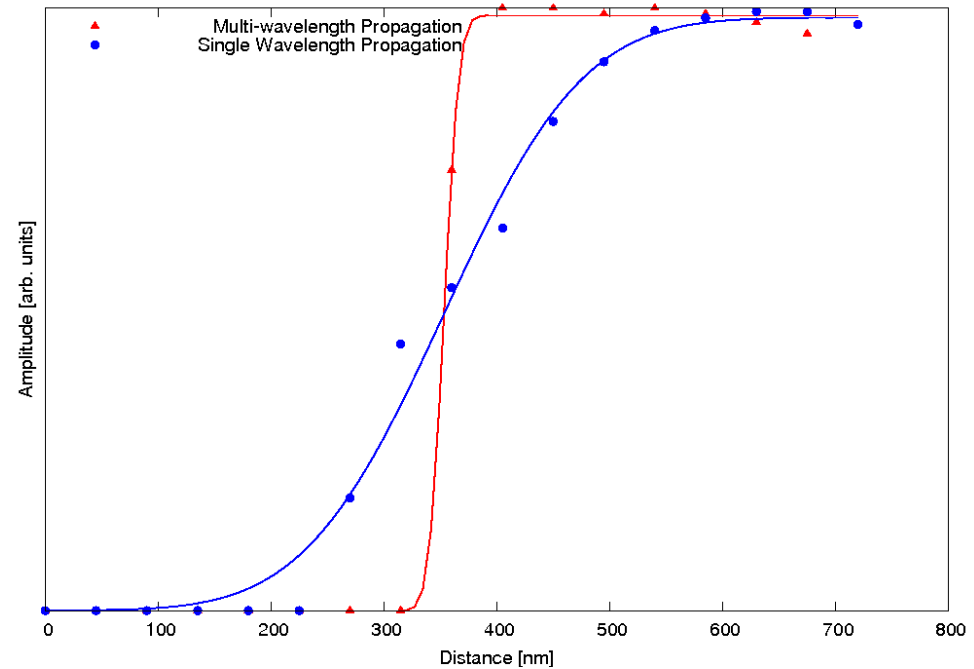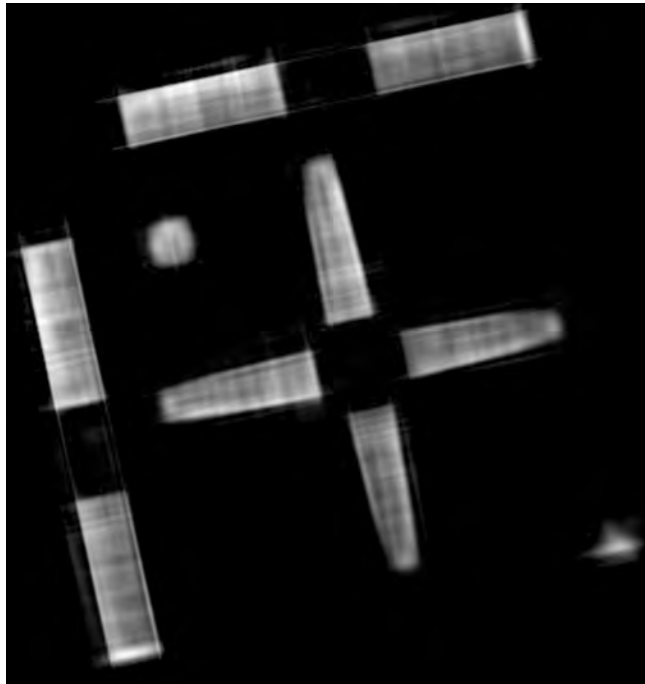
Explicit propagation of frequency components achieved using a loose support, with greatly improved resolution of the edges of the figure compared with conventional CDI.

Conclusions

- Generalization of X-ray imaging to incorporate coherence properties of X-ray wavefields.

- Modal expansion approach incorporates partial spatial coherence of quasi-monochromatic fields, or the spectral structure of spatially-coherent polychromatic fields.

- Computationally efficient, involves only Fresnel propagation of two-dimensional modes.

- Advantages even if illumination has high spatial coherence.

- Can be adopted to model general $W(\mathbf{r}_1, \mathbf{r}_2, \omega)$.

Acknowledgements

The Centre of Excellence for Coherent X-ray Science is funded by the Australian Research Council

- Keith Nugent, Ruben Dilanian, David Vine, Bo Chen, Sam Flewett, Lachlan Whitehead(Melbourne)

- Garth Williams (now at SLAC)

- Andrew Peele, Chanh Tran, Jesse Clarke, Corey Putkunz (Latrobe)

- Brian Abbey (now at Oxford)

- Ian McNulty (APS Argonne)